THE JOURNAL OF BIOLOGICAL CHEMISTRY VOL. 287, NO. 36, pp. 30529–30540, August 31, 2012

Mapping Functional Interactions in a Heterodimeric Phospholipid Pump*

Received for publication, April 11, 2012, and in revised form, July 6, 2012 Published, JBC Papers in Press, July 12, 2012, DOI 10.1074/jbc.M112.371088

Catheleyne F. Puts[‡1], Radhakrishnan Panatala[‡1], Hanka Hennrich[‡1], Alina Tsareva[§], Patrick Williamson[§], and Joost C. M. Holthuis[‡¶2]

From the [‡]Department of Membrane Enzymology, Bijvoet Center and Institute of Biomembranes, Utrecht University, The Netherlands, the [§]Department of Biology, Amherst College, Amherst, Massachusetts 01002, and the [¶]Molecular Cell Biology Division, University of Osnabrück, 49076 Osnabrück, Germany

Background: P_4-ATPases form heterodimeric complexes with Cdc50 proteins and catalyze phospholipid transport to generate membrane asymmetry.
Results: Disruption of disulfide bridges in the ectodomain of Cdc50 proteins has reciprocal effects on P_4-ATPase binding and phospholipid transport.
Conclusion: Cdc50 proteins are critical components of the P_4-ATPase flippase machinery.
Significance: Our data begin to define the function of different regions of the Cdc50 polypeptide in supporting P_4-ATPase-catalyzed phospholipid transport.

Type 4 P-type ATPases (P_4-ATPases) catalyze phospholipid transport to generate phospholipid asymmetry across membranes of late secretory and endocytic compartments, but their kinship to cation-transporting P-type transporters raised doubts about whether P_4-ATPases alone are sufficient to mediate flippase activity. P_4-ATPases form heteromeric complexes with Cdc50 proteins. Studies of the enzymatic properties of purified P_4-ATPase·Cdc50 complexes showed that catalytic activity depends on direct and specific interactions between Cdc50 subunit and transporter, whereas *in vivo* interaction assays suggested that the binding affinity for each other fluctuates during the transport reaction cycle. The structural determinants that govern this dynamic association remain to be established. Using domain swapping, site-directed, and random mutagenesis approaches, we here show that residues throughout the subunit contribute to forming the heterodimer. Moreover, we find that a precise conformation of the large ectodomain of Cdc50 proteins is crucial for the specificity and functionality to transporter/subunit interactions. We also identified two highly conserved disulfide bridges in the Cdc50 ectodomain. Functional analysis of cysteine mutants that disrupt these disulfide bridges revealed an inverse relationship between subunit binding and P_4-ATPase-catalyzed phospholipid transport. Collectively, our data indicate that a dynamic association between subunit and transporter is crucial for the transport reaction cycle of the heterodimer.

The P-type ATPases are a large and ancient family of cation-transporting membrane pumps. Well known representatives are the Na^+/K^+-ATPase, which generates electrochemical gradients for Na^+ and K^+ ions, and the Ca^{2+}-ATPase SERCA, which pumps cytosolic Ca^{2+} ions into the lumen of the sarcoplasmic reticulum. Transport by P-type ATPases follows a cyclic scheme of conformational changes in which the pump sequentially opens substrate binding sites to the cytoplasm (the E_1 conformations) and exoplasmic surface (the E_2 conformations). This cycle is driven by transient phosphorylation of the ATPase at a highly conserved aspartate residue, hence the designation P-type (1, 2). Although P-type ATPases usually pump small cations or metal ions, members of the P_4 subfamily are implicated in transport of the much larger phospholipids (3–5) creating phospholipid asymmetry in membranes of late secretory and endocytic compartments (6–8). Their sequence homology and common domain organization with other P-type ATPases suggest that P_4-ATPases[3] utilize a transport mechanism that rests on the same principles and structural elements (1, 9, 10). Although cation-transporting P-type ATPases utilize a spatially restricted ion-binding pocket in the center of the transmembrane domain, residues both inside and outside this canonical binding pocket have been implicated in phospholipid substrate specificity of P_4-ATPases (11, 12). How the transport mechanism of P-type cation pumps is adapted in P_4-ATPases to translocate phospholipids is poorly understood.

Besides their unusual substrate, there is another feature that sets P_4-ATPases apart from most other P-type pumps, namely their association with an obligatory subunit, the Cdc50 protein. This hallmark is shared by only one other subfamily of P-type pumps, namely P_{2C}-ATPases, comprising Na^+/K^+- and H^+/K^+-ATPases, which associate with an unrelated β-subunit. Association with the β-subunit in P_{2C}-ATPases affects protein

* This work was supported by grants from the European Union Framework V Program (the Flippase Project), the Dutch Organization of Sciences (NWO-CW), the Utrecht High Potential Program (to J. C. M. H.), and the National Science Foundation (to P. W.).
[1] These authors contributed equally to this work.
[2] To whom correspondence should be addressed: Molecular Cell Biology Division, University of Osnabrück, Barbarastr. 13, 49076 Osnabrück, Germany. Tel.: 49-541969-7140; Fax: 49-541969-2884; E-mail: holthuis@uos.de.

[3] The abbreviations used are: P_4-ATPase, type 4 P-type ATPase; SD, synthetic dextrose; Cub, C-terminal half of ubiquitin; mPEG, methoxypolyethylene glycol-5000 maleimide; NBD, nitrobenzoxadiazole; Nub, N-terminal half of ubiquitin; PC, phosphatidylcholine; PE, phosphatidylethanolamine; PS, phosphatidylserine; Pap B, papuamide B.

folding, membrane insertion, plasma membrane delivery, and activity of the enzyme (13).

Compared with their P-type ATPase-binding partners, Cdc50 and β-subunits are relatively small. They arose independently during evolution and show little if any sequence homology (14). Nevertheless, both the β-subunit and Cdc50 have substantial ectodomains that contain multiple glycosylation sites and highly conserved cysteine residues, capable of forming one or more disulfide bridge (10).

Yeast contains five different P_4-ATPases that are located in late secretory and endocytic organelles (*i.e.* Dnf1 and Dnf2 at the plasma membrane, Dnf3 and Drs2 at the *trans*-Golgi network, and Neo1 in endosomes) (6, 15, 16). The yeast Cdc50 proteins Cdc50, Lem3, and Crf1 form heteromeric complexes with Drs2, Dnf1/Dnf2, and Dnf3, respectively (18–20). Formation of these complexes is required for stabilization and ER export of either partner (8, 17, 18, 20). A similar relationship has been observed in other organisms as well. For example, human class-1 P_4-ATPases also require association with a Cdc50 subunit for ER export and to reach their final subcellular destination (21, 22, 23).

In recent studies, we and others showed that catalytic activity of P_4-ATPases critically relies on association with a Cdc50 subunit (19, 22, 24–26). Using a genetic reporter system, we also found that the affinity of P_4-ATPases for their Cdc50 binding partners fluctuates during the transport reaction cycle, being strongest at the E_2P state, where phospholipid is loaded onto the enzyme (19). Together, these results suggested that Cdc50 proteins play an intimate role in P_4-ATPase-catalyzed phospholipid transport. To further elucidate the inner workings of these heterodimeric lipid pumps, we here set out to map functional interactions between P_4-ATPases and their Cdc50 binding partners in yeast.

EXPERIMENTAL PROCEDURES

Yeast Strains and Plasmids—Yeast strains used for the split-ubiquitin assay were THY.AP4 (MATa ura3 leu2 lexA::lacZ::trp1 lexA::HIS3 lexA::ADE2) and THY.AP5 (MATα URA3 leu2 trp1 his3 loxP::ade2). The Δ*cdc50* and Δ*lem3* deletion mutants were created in yeast strain SEY6210 (MATα ura3-52 his3-Δ200 leu2–3,112 trp1-Δ901 lys2-801 suc2-Δ9) using a loxP-HIS3-loxP cassette (6, 19). All strains were grown in synthetic dextrose (SD) medium. Plasmids used for the split-ubiquitin assay were created as described (19). In brief, constructs containing the C terminus of ubiquitin (Cub) were generated in THY.AP4 by *in vivo* recombination between the linearized vector pMetYCgate and PCR fragments of Drs2, Dnf1, and Dnf3, respectively. Constructs containing the N terminus of ubiquitin (Nub) were created in THY.AP5 by *in vivo* recombination between the linearized vector pNXgate33–3HA and PCR fragments of Cdc50, Crf1, and Lem3, respectively. The resulting transporter-Cub and Nub-Cdc50 subunit constructs were reisolated and sequenced to verify fidelity of recombination. The Nub-Lem3 construct was subjected to random mutagenesis using 70 mg/ml hydroxylamine hydrochloride (75 °C, pH 6.6). The mutagenized construct was purified by agarose gel electrophoresis and transformed into THY.AP4 harboring the Dnf1-Cub construct. Nub-Lem3 interaction mutants were analyzed for protein expression levels by immunoblotting, isolated, sequenced, and then reanalyzed for interaction with Dnf1-Cub using the split-ubiquitin assay (see below). For the generation of Cdc50·Crf1 chimeras, Cdc50 and Crf1 were divided into five topological domains: namely two transmembrane domains predicted by TMHMM 2.0 (27), two cytosolic tails, and the large ectodomain. To create chimeras between the Cdc50 and Crf1 ectodomains, their sequences were aligned using ClustalW2 (28). Two swapping sites in regions of high sequence identity were selected to divide the ectodomain into three roughly equal parts. Chimeras were assembled by fusion PCR and then cloned into pNXgate33–3HA. Cysteine-to-alanine substitutions were created by site-directed mutagenesis of Nub-Cdc50, Nub-Crf1, and Nub-Lem3 in pNXgate33–3HA or Lem3-Myc_9 in pRS425 under control of the PMA1 promotor (19). All constructs were sequence-verified and transformed into THY.AP4 for split-ubiquitin assays or into Δ*cdc50* and Δ*lem3* mutant strains for drug sensitivity and NBD-phospholipid transport studies.

Split-ubiquitin Assays—The mating-based split-ubiquitin assay of Obrdlik *et al.* (29) was used as described (19). For interaction assays, mated Cub and Nub strains were selected for diploids, which were replicated on SD−Leu−Trp−His−Ade plates to test for growth. Sensitivity of these growth assays was determined by methionine-controlled expression of the Cub constructs. For quantitative assays of β-galactosidase expression, diploids were grown overnight in SD−Leu−Trp suspension cultures at 30 °C to midlogarithmic growth phase. The culture medium of cells expressing either Drs2-Cub and Dnf1-Cub or Dnf3-Cub was supplemented with 75 and 40 μM methionine, respectively, to ensure equal expression of the transporters. One A_{600} of each culture was harvested, permeabilized in 100 μl of YPER permeabilization reagent (Pierce) for 20 min at room temperature, and then combined with 1 ml of Z buffer (60 mM Na_2HPO_4, 40 mM NaH_2PO_4, 10 mM KCl, 1 mM $MgSO_4$, pH 7.0) containing 4 mg/ml freshly added *o*-nitrophenyl-β-D-galactopyranoside. After incubation at 30 °C for 10 min, the assay mixture was sedimented, and the A_{420} of the supernatant was measured to obtain specific activity for β-galactosidase.

Mapping of Disulfide Bridges in Cdc50 Ectodomain—THY.AP4 cells expressing wild type or cysteine mutants of Nub-tagged Cdc50 proteins were grown at 30 °C to midlogarithmic phase in selective SD medium, resuspended in ice-cold TEPI buffer (100 mM Tris-HCl, pH 7.5, 10 mM EDTA, 1 μg/ml apoprotein, 1 μg/ml leupeptin, 1 μg/ml pepstatin, 5 μg/ml antipain, 157 μg/ml benzamidine), and lysed by bead bashing. After clearing lysates for unbroken cells and nuclei (700 × g_{av}, 5 min, 4 °C), membranes were collected by centrifugation at 100,000 × g_{av} (1 h, 4 °C), resuspended in SDS/urea sample buffer, and normalized for protein content. To break disulfide bridges, extracts were incubated with 5 mM dithiothreitol (DTT) for 20 min at 37 °C. For modification of free cysteines, extracts were incubated with methoxypolyethylene glycol-5000 maleimide (mPEG; Sigma-Aldrich) at the indicated concentration for 20 min at 37 °C. Next, samples were supplemented with 10 mM *N*-ethylmaleimide, incubated for another 20 min at 37 °C, and subjected to SDS-gel electrophoresis and immuno-

blot analysis using anti-HA antibody (12CA5; Santa Cruz Biotechnology, Inc., Santa Cruz, CA).

Drug Sensitivity Assays—Yeast Δ*cdc50* and Δ*lem3* mutant strains transformed with wild type or mutant Cdc50 expression constructs were grown at 30 °C in selective SD medium to midlogarithmic phase. Serial dilutions of cell suspensions were spotted onto SD plates supplemented with 1 μM papuamide B (Flintbox, Wellspring Worldwide, Chicago, IL) or DMSO as a control. Alternatively, cell suspensions of 0.2 A_{600}/ml were spotted onto SD plates containing concentration gradients of miltefosine (0–5 μg/ml; Sigma-Aldrich) or duramycin (0–25 μg/ml; Santa Cruz Biotechnology, Inc.). Plates were incubated at 30 °C, and growth was monitored after 2–3 days.

NBD-lipid Uptake—Palmitoyl-(NBD-hexanoyl)-PE (NBD-PE) and palmitoyl-(NBD-hexanoyl)-PC (NBD-PC) were from Avanti Polar Lipids (Birmingham, AL). NBD-lipid stocks (10 mM) were prepared in DMSO. NBD-lipid uptake experiments were performed essentially as described (6), with some modifications. In brief, cells were grown to midlogarithmic phase, resuspended in SD medium to 10 A_{600}/ml, and incubated for 20 min at 30 °C with 50 μM NBD-PE or NBD-PC. NBD-labeled cells were washed twice in ice-cold SD medium without glucose but containing 2% sorbitol and 20 mM NaN_3 (SSA medium) supplemented with 4% (w/v) BSA, resuspended in ice-cold SSA medium, and labeled with propidium iodide. Flow cytometry of NBD-labeled cells was performed on a FACSCalibur flow cytometer (BD Biosciences) equipped with an argon laser using Cell Quest software, as described (6). A histogram of the red fluorescence (propidium iodide; SP 610, LP 630) was used to set the gate that excluded dead cells from the analysis. Green fluorescence (NBD; SP 560, BP 515–545) of living cells was plotted on a histogram. The mean fluorescence intensity was calculated and used for further statistical analysis.

RESULTS

Residues Critical for P_4-ATPase Binding Are Located throughout Topologically Distinct Cdc50 Domains—The critical role of Cdc50 subunits in P_4-ATPase function emphasizes the importance of understanding how the two proteins interact. The example of the transporter/subunit interaction deduced from a recently solved crystal structure of the Na^+/K^+-transporting P_{2C}-ATPase·β-subunit complex (30) would suggest an intimate interaction encompassing a large interacting surface, but the highly dynamic nature of the interaction between P_4-ATPases and Cdc50 subunits (19) might suggest a smaller, more discrete area of contact. To investigate how P_4-ATPases and Cdc50 subunits interact, we took advantage of the split-ubiquitin system (29, 31). The P_4-ATPase transporter was tagged with the Cub linked to a transcriptional activator as a reporter, whereas the Cdc50 subunit was marked with the Nub (Fig. 1*A*). Previous experiments have shown that specific interaction between the transporter and subunit in living yeast results in release of the reporter; the subsequent transcriptional activations confer the ability to grow in the absence of histidine and adenine, detectable by growth assays, and activate the production of β-galactosidase, which can be measured quantitatively in cell extracts (19).

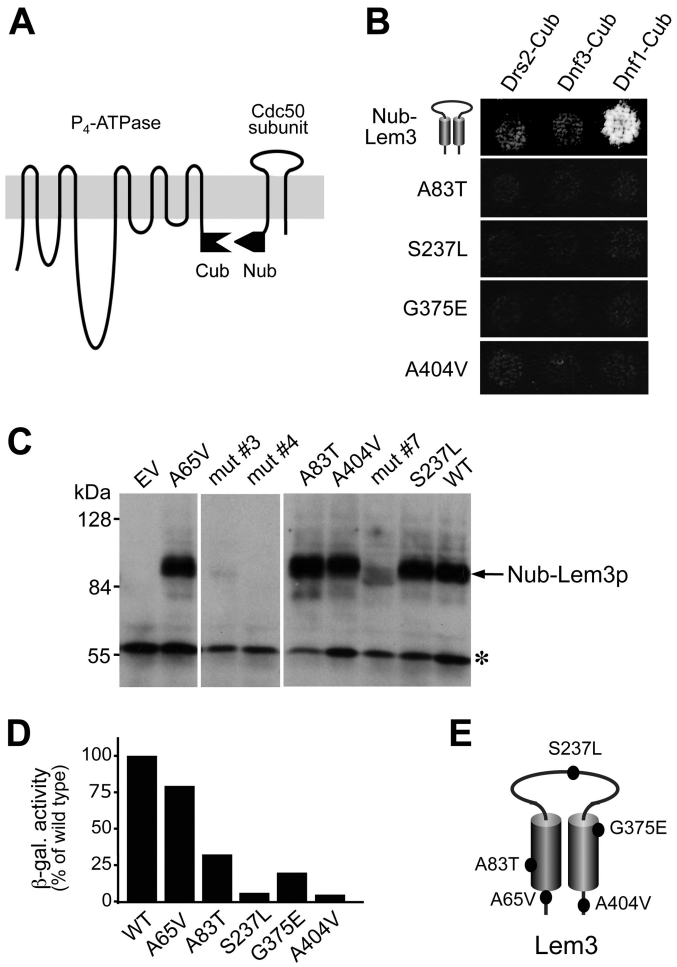

FIGURE 1. **Residues critical for P_4-ATPase·Cdc50 interactions are spread throughout the Cdc50 subunit.** *A*, schematic representation of a Cub-tagged P_4-ATPase and Nub-tagged Cdc50 subunit. *B*, split-ubiquitin growth assay reporting interactions of Dnf1-Cub with wild type (*WT*) and single-point mutants of Nub-Lem3. *C*, immunoblot analysis of membrane extracts from equal amounts of yeast cells expressing WT or mutant Nub-Lem3 using an antibody recognizing the HA-epitope encoded in the Nub tag. *D*, quantitative measurement of Dnf1-Cub interactions with WT or mutant Nub-Lem3 using the split-ubiquitin β-galactosidase assay. *E*, positions of single point mutations in Lem3 having an impact on Dnf1 binding.

To map the parts of the subunits that interact with the transporter, plasmid DNA containing the gene for a Nub-tagged Lem3 subunit was mutagenized *in vitro* by treatment with hydroxylamine. The extent of mutagenesis was monitored by measuring the decrease in transformation efficiency (data not shown); DNA was treated until this efficiency dropped 30-fold and then purified; restriction analysis indicated that the DNA was intact and recovered in high yield. This DNA was then used to transform yeast harboring the Cub-tagged cognate transporter Dnf1. Transformants that failed to grow in the absence of histidine and adenine were identified by replica plating. Expression of Nub-Lem3 in such transformants was verified by immunoblotting using an antibody against a C-terminal HA epitope present in the Nub-tagged protein. One common phenotype of these mutants was the absence or very low concentration of the Nub-tagged subunit in cells (*e.g.* mutants 3, 4, and 7; Fig. 1*C*). Mutants in which the level of expression of the subunit was disrupted were set aside. We concentrated on

mutants with strongly reduced interaction (Fig. 1*B*) and subunit protein levels comparable with those of wild type cells (Fig. 1*C*). The mutated plasmids in transformants with this phenotype were isolated and sequenced. As expected, some mutations were observed in the Nub tag itself (data not shown). However, there were also several instances where mutations occurred exclusively in the subunit structural gene. For these mutations, the interaction efficiency was estimated by quantitative comparison of the level of β-galactosidase activity and the amount of the Nub-tagged subunit, as determined by immunoblot analysis. The results of these measurements are shown in Fig. 1*D*. These mutations have two characteristics. One is that they are scattered throughout the protein, including the cytoplasmic domain and ectodomain as well as the transmembrane helices (Fig. 1*E*), indicating that the subunit interacts with the transporter over a large surface rather than at a small binding domain. The second is that they tend to occur in highly conserved residues. This finding suggests that these residues contribute to binding between subunits and transporters in general. Because these mutants were selected for reduced interaction with the transporter Dnf1, we investigated this latter possibility by testing whether these mutants were also less able to interact with the transporter Dnf2. As predicted from the sequence conservation of the affected residues, interactions with Dnf2 were also reduced (data not shown).

Although the residues identified by random mutagenesis may be generally necessary for interaction between subunits and transporters, they cannot be sufficient, because the various subunits are not capable of strong interactions with all of the P_4-ATPases that they encounter; the subunits Cdc50 and Crf1 contain these amino acids but do not interact strongly with either Dnf1 or Dnf2, and Lem3 does not interact strongly with Dnf3 or Drs2. This led us to investigate where in the subunit the determinants for transporter-specific interactions are located.

The Ectodomain of Cdc50 Subunits Mediates P_4-ATPase Binding Specificity—Co-immunoprecipitation analysis showed that the yeast subunits Cdc50, Crf1, and Lem3 associate with the P_4-ATPases Drs2, Dnf3, and Dnf1/2, respectively (17, 18). We have been able to recapitulate these specific interactions using the split-ubiquitin assay (19) (Fig. 2*A*). Whereas the Dnf1·Lem3 and Dnf2·Lem3 complexes reside at the plasma membrane, the Drs2·Cdc50 and Dnf3·Crf1 complexes co-localize in the *trans*-Golgi network (6, 8, 15, 17). To investigate whether any one domain of the subunit controls specificity to P_4-ATPase binding, we generated a series of chimeric constructs, in which topologically distinct domains of Cdc50 and Crf1 proteins were exchanged. We then analyzed the specificity of the interaction of these chimeras with Drs2 and Dnf3 using the split-ubiquitin assay. Dnf1 served as a negative control. As shown in Fig. 2*B*, swapping of cytosolic tails, membrane spans, or both had no impact on binding specificity. In contrast, swapping the ectodomain that connects the two membrane spans of each subunit caused a complete switch in P_4-ATPase binding specificity. Thus, a chimera consisting of the cytosolic tails and membrane spans of Cdc50 fused to the ectodomain of Crf1 interacted specifically with Dnf3, whereas its reverse counterpart associated exclusively with Drs2 (Fig. 2*B*). These results

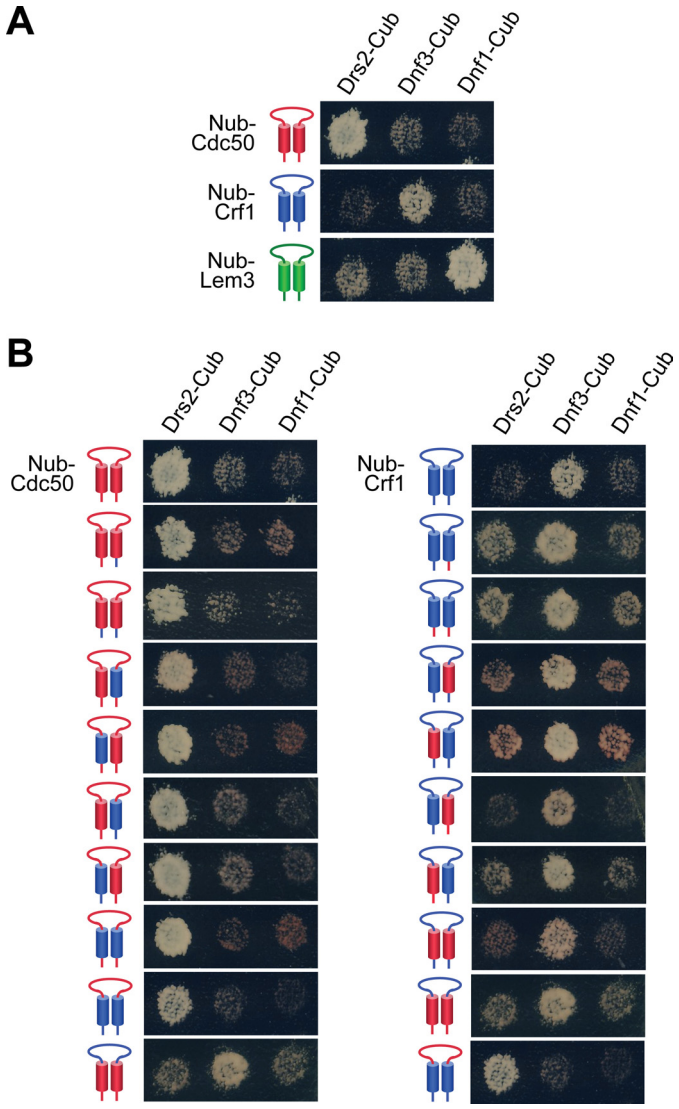

FIGURE 2. **The ectodomain of Cdc50 subunits is a key determinant of P_4-ATPase binding specificity.** *A*, split-ubiquitin growth assay reporting specific interactions between Drs2-Cub, Dnf3-Cub, Dnf1-Cub, and their cognate Nub-Cdc50 subunits. *B*, split-ubiquitin growth assay reporting interactions between Nub-Cdc50·Crf1 chimeras and Cub-tagged P_4-ATPases. Cdc50- and Crf1-derived domains are marked in *red* and *blue*, respectively.

demonstrate that the ectodomain of the subunits is the critical determinant of P_4-ATPase binding specificity.

A Precise Configuration of the Cdc50 Ectodomain Is Essential for P_4-ATPase Binding—We next investigated whether we could narrow the location of the determinants of P_4-ATPase binding specificity to a discrete region of the Cdc50 ectodomain. To this end, the ectodomains of Cdc50 and Crf1 were divided in three roughly equal parts (Fig. 3), and a new series of chimeric constructs was created, in which individual ectodomain segments were exchanged. All junctions were located in regions where Cdc50 and Crf1 sequences were identical. Expression of chimeras was verified by immunoblot analysis using an antibody against the C-terminal HA epitope. As shown in Fig. 4*A*, the majority of these chimeras lost the ability to bind either Drs2 or Dnf3, suggesting that they failed to fold into a conformation capable of interacting with the transporter. Chimeras carrying an ectodomain in which the first one-third was

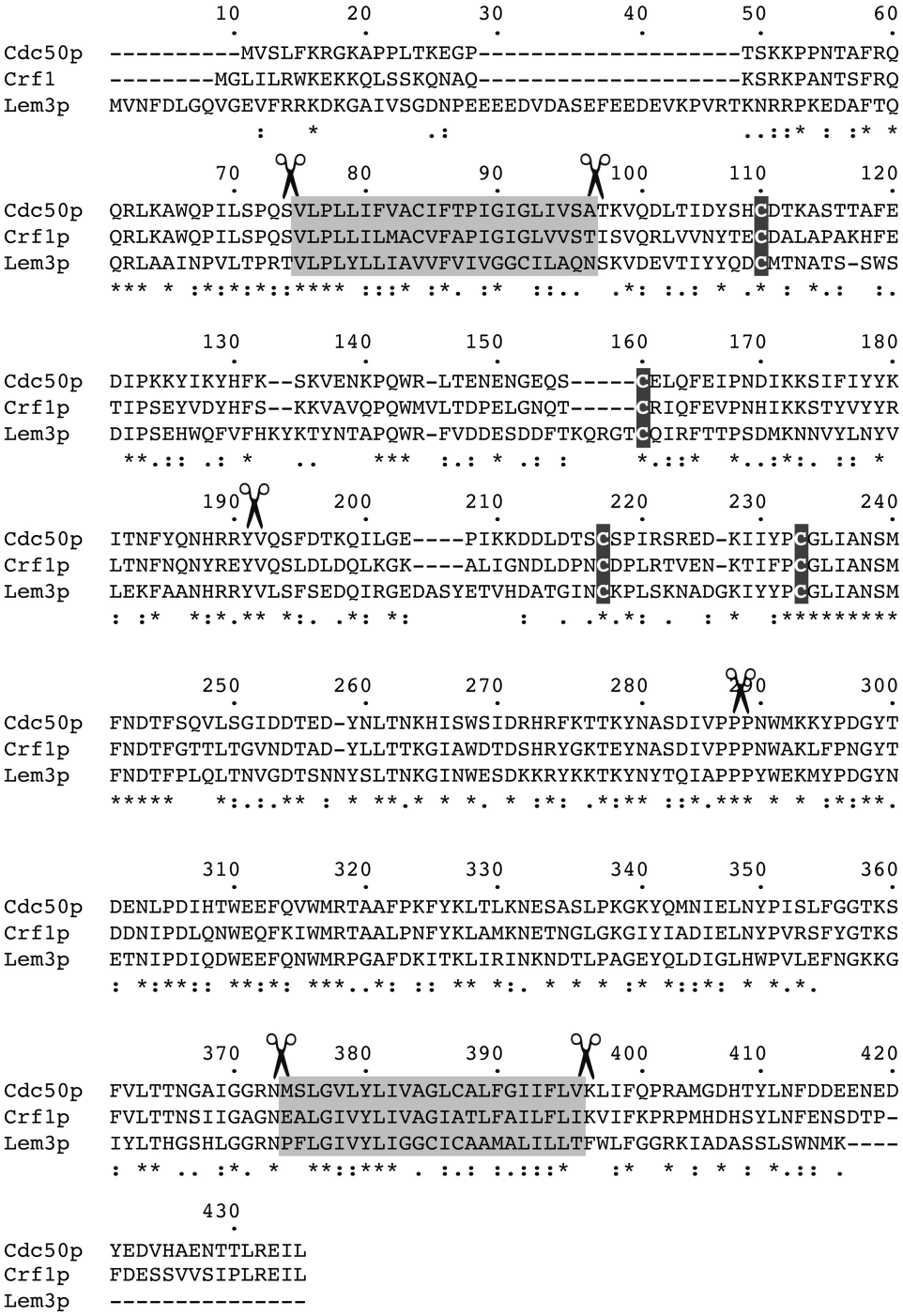

FIGURE 3. **Sequence alignment of yeast Cdc50 proteins.** Shown is a multisequence alignment generated by the ClustalW2 algorithm. The *asterisks* mark amino acid residues conserved in all three family members. Transmembrane domains predicted by the TMHMM prediction server are *shaded* in *gray*. Conserved cysteine residues in the Cdc50 ectodomain are *shaded* in *black*. *Scissors* indicate the swapping sites that were used to create the Cdc50·Crf1 chimeras analyzed in this study.

derived from Cdc50 and the remainder from Crf1 formed a notable exception. Interestingly, these chimeras lost the ability to discriminate between Drs2 and Dnf3 and bound both transporters with similar affinity (Fig. 4*A*, *row 5*); moreover, this result was observed whether the ectodomain was associated with the cytosolic tails and membrane spans of Crf1 (*right*) or Cdc50 (*left*). These observations were confirmed by quantitative measurements of β-galactosidase activity (Fig. 4*B*). Together, these data suggest that the first third of the ectodomain has critical determinants for Cdc50·Drs2, but not for Crf1·Dnf3 binding. Our previous work revealed that Drs2/Cdc50 interactions are coupled to the ATPase reaction cycle and that Cdc50 preferentially interacts with the E_2P phosphoenzyme intermediate of Drs2 (19). Interestingly, the Crf1-based chimera carrying the first one-third of the ectodomain of Cdc50 displayed the same reaction cycle-dependent association with Drs2, interacting strongly with a mutant blocked at the E_2P step (E342Q) but failing to interact with mutants blocked before the

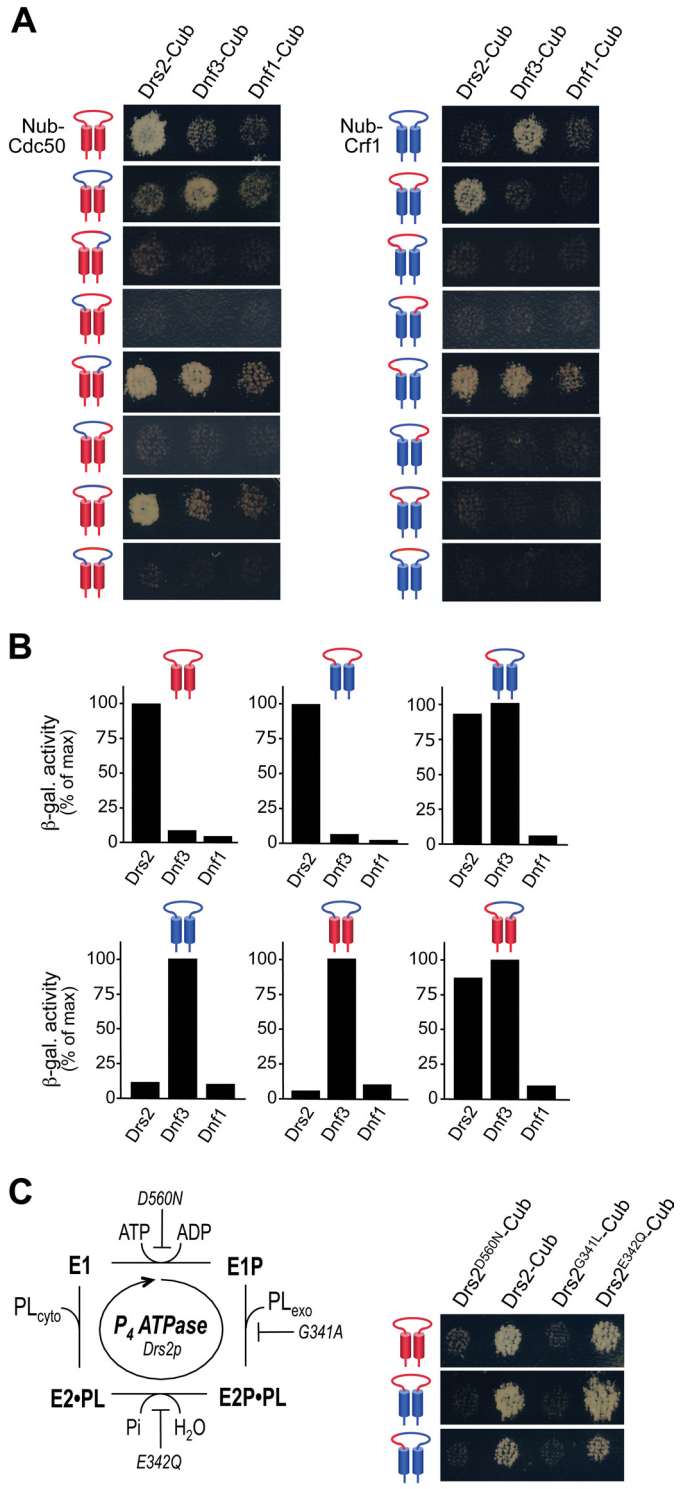

FIGURE 4. **A precise configuration of the Cdc50 ectodomain is critical for P_4-ATPase binding.** *A*, split-ubiquitin growth assay reporting interactions between Nub-Cdc50·Crf1 chimeras and Cub-tagged P_4-ATPases. *B*, quantitative measurements of Nub-Cdc50·Crf1 chimeras with Cub-tagged P_4-ATPases using the split-ubiquitin β-galactosidase assay. For normalizing expression levels of Cub-tagged P_4-ATPases, measurements were performed on cells grown in the presence of 75 μM (Drs2-Cub, Dnf1-Cub) or 40 μM methionine (Dnf3-Cub). *C*, schematic representation of the P_4-ATPase reaction cycle. Residues important for $E_1 \rightarrow E_1P$, $E_1P \rightarrow E_2P$, and $E_2P \rightarrow E_2$ transitions in Drs2 are indicated. *D*, split-ubiquitin growth assay reporting interactions between Nub-Cdc50·Crf1 chimeras and Drs2-Cub, $Drs2^{D560N}$-Cub, $Drs2^{E342Q}$-Cub, and $Drs2^{G341L}$-Cub.

E_2P step (D560N, blocked at E_1, and G341L, blocked at E_1P) (Fig. 4*C*). However, the presence of this region was not sufficient for Drs2 binding (Fig. 4*A*), indicating that it did not act autonomously. Together, these data indicate that several regions within the subunit's ectodomain must cooperate to convey binding specificity, making the precise conformation of the Cdc50 ectodomain of critical importance for P_4-ATPase·Cdc50 complex assembly.

Ectodomain-mediated Binding of Cdc50 Subunits Is Required but Not Sufficient for P_4-ATPase Function—Characterization of the enzymatic properties of Drs2·Cdc50 complexes purified from yeast revealed that catalytic activity relies on direct interactions between subunit and transporter (19). The availability of chimeric Cdc50 subunits with altered binding properties provided a novel opportunity to further explore the functional relationship between P_4-ATPases and Cdc50 subunits. Loss of Drs2 renders yeast cells hypersensitive to papuamide B (Pap B), a cyclic lipopeptide that exerts its cytolytic activity through binding to PS exposed on the cell surface (32). This phenotype is consistent with Drs2-catalyzed PS transport from the exoplasmic to the cytosolic membrane leaflet (5). Cells lacking Cdc50 also display hypersensitivity toward Pap B (8), consistent with a requirement of Cdc50 for Drs2 function. Pap B hypersensitivity in the Δ*cdc50* mutant was suppressed by expression of Nub-tagged Cdc50 (Fig. 5, *top left panel*). Nub-Cdc50·Crf1 chimeras that lost the ability to bind Drs2 consistently failed to suppress Pap B hypersensitivity, as expected if subunit binding is essential for Drs2 function. However, the pair of Cdc50·Crf1 chimeras that retained their Drs2-binding properties but lost the ability to discriminate between Drs2 and Dnf3 provide an interesting case. The chimera containing Crf1 sequences only in the C-terminal two-thirds of the ectodomain bound to both transporters and suppressed Pap B hypersensitivity in Δ*cdc50* cells (Fig. 5, *left*). This result shows that, although binding of a subunit is critical, binding specificity is dispensable for transporter function. In contrast, the chimera consisting of Crf1 except for the first third of the ectodomain was also able to bind Drs2 yet failed to suppress Pap B hypersensitivity (Fig. 5, *right*). Importantly, the latter finding shows that association with a Cdc50 subunit, although required, is not sufficient for P_4-ATPase function.

The inactive Crf1-based chimera containing the first one-third of the Cdc50 ectodomain provided a starting point for further exploration of the structural basis for functional transporter/subunit interactions. In particular, we found that introducing either the N-terminal or C-terminal transmembrane and cytosolic domains into the inactive Crf1-based chimera were sufficient to restore functionality, as evidenced by the Pap B sensitivity assay (Fig. 6*B*). Neither substitution had any obvious impact on the affinity or specificity of transporter binding (Fig. 6*A*). These results indicate that a loss in function associated with an imperfect configuration of the Cdc50 ectodomain can be compensated by structural information contained within the subunit's membrane spans and/or cytosolic tails. This result implies that the several domains of Cdc50 subunits not only contribute binding residues but also cooperate to render transporter/subunit interactions functional.

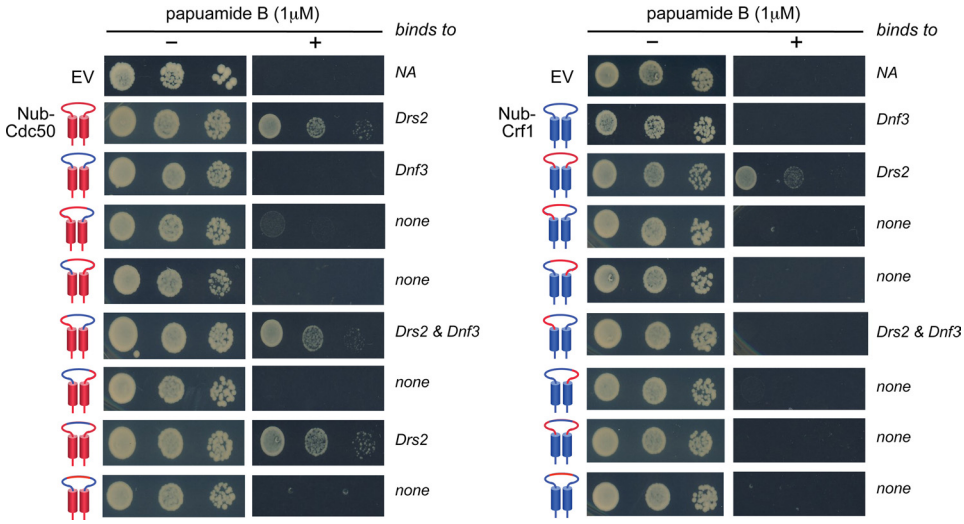

FIGURE 5. **Ectodomain-mediated binding of Cdc50 subunits is required but not sufficient for P_4-ATPase function.** Serial dilutions of a Δ*cdc50* mutant strain transfected with empty vector (*EV*), Nub-Cdc50, Nub-Crf1, or a Nub-Cdc50·Crf1 chimera were spotted onto SD plates containing DMSO (−) or 1 μM papuamide B in DMSO (+) and incubated at 30 °C for 2 days.

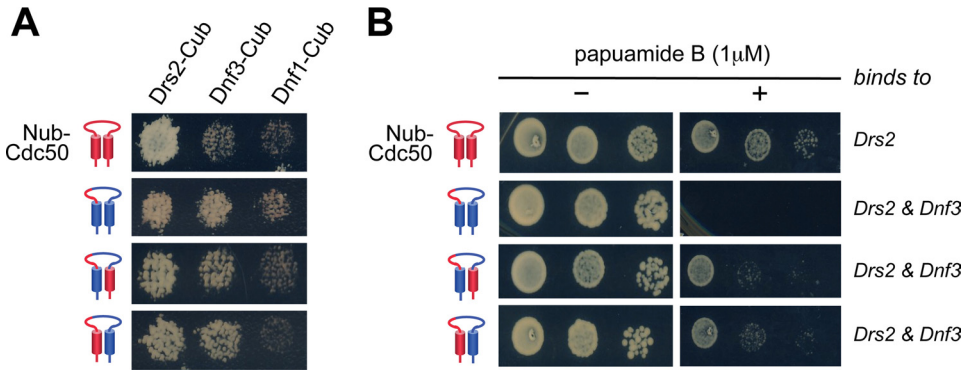

FIGURE 6. **Cdc50 function relies on cooperation between topologically distinct domains.** *A*, split-ubiquitin growth assay reporting interactions between Nub-Cdc50·Crf1 chimeras and Cub-tagged transporters. *B*, a Δ*cdc50* mutant strain transfected with Nub-Cdc50 or a Nub-Cdc50·Crf1 chimera was analyzed for papuamide B sensitivity as in Fig. 4.

The Ectodomain of Cdc50 Subunits Contains Two Conserved Disulfide Bridges—The ectodomain of Cdc50 subunits in yeast contains four highly conserved cysteine residues (Fig. 3). At least two of these are paired to form an intramolecular disulfide bridge; wild type Nub-tagged Cdc50 displays a marked SDS-PAGE mobility shift following exposure to the reducing agent DTT (Fig. 7*A*, *lanes 1* and *2* in the *top two rows*). A similar shift can be observed in wild type Nub-tagged Crf1 and Lem3 (Fig. 7*A*, *lanes 1* and *2* in the *bottom four rows*). Because even subtle changes in the configuration of Cdc50 ectodomains can disrupt transporter binding and function (Figs. 5 and 6), we first set out to identify the cysteines responsible for disulfide bridge formation. To this end, single cysteine residues or pairs of cysteine residues in the ectodomain of Nub-tagged subunits were replaced by alanine residues. In Nub-Cdc50, mutation of Cys^{80}, Cys^{123}, or both abolished the DTT-induced mobility shift (Fig. 7*A*, *top row*), implying that these cysteine residues pair to form the disulfide bridge responsible for the mobility shift. In contrast, mutation of the C-terminal cysteine pair Cys^{176}-Cys^{190} left the mobility shift intact (Fig. 7*A*, *row 2*). Mutation of the corresponding cysteine residues in Nub-Crf1 and Nub-Lem3 gave similar results (Fig. 7*A*, *rows 3–6*), indicating that a disulfide bridge between the N-terminal pair of cysteine residues is a conserved feature of yeast Cdc50 subunits.

The spacing between the C-terminal pair of cysteine residues in the subunit's ectodomain is quite small (13–14 residues), so that a disulfide bridge between this pair may not produce a mobility shift that is large enough to resolve by SDS-PAGE. We therefore used a different approach to investigate whether the C-terminal pair of cysteine residues also forms a disulfide bond. In these experiments, wild type and mutant subunits in SDS/urea-solubilized membrane extracts were treated with mPEG to tag free cysteine residues with a 5-kDa PEG moiety prior to immunoblot analysis. SDS-gel analysis of wild type Nub-Cdc50 revealed singly and doubly tagged mobility-shifted mPEG adducts (Fig. 7*B*, *left*), consistent with the presence of two free but poorly reactive cysteine residues in the hydrophobic membrane spans of Cdc50 (Cys^{54} and Cys^{343}; see Fig. 3). When the N-terminal disulfide pair in Cdc50 is disrupted by the C80A mutation, tagging with mPEG resulted in only multiply tagged proteins (Fig. 7*B*, *middle panel*, *top two arrowheads*) and the virtual disappearance of the singly tagged species (*bottom arrowhead*), as expected if the C80A mutation generates a highly reactive third cysteine (Cys^{123}) available to react with

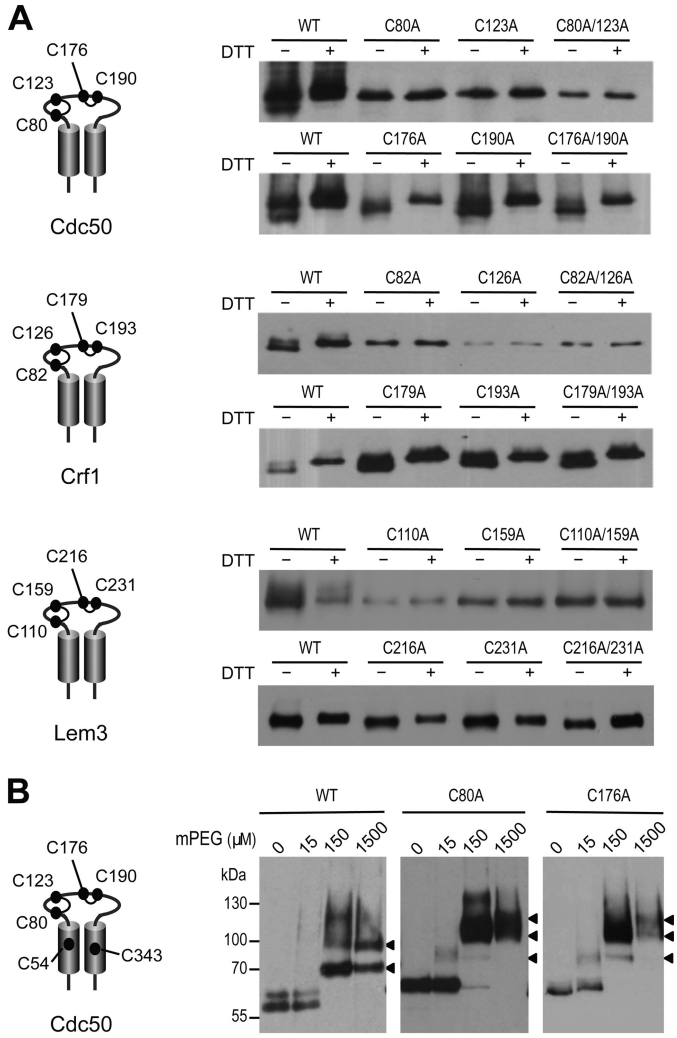

FIGURE 7. **Cdc50 proteins contain two highly conserved disulfide bridges.** *A*, membrane extracts of yeast cells expressing wild type (*WT*) or mutant Nub-Cdc50 carrying one or two cysteine-to-alanine substitutions in the ectodomain were processed for immunoblotting in the presence (+) or absence of DTT (−). Blots were stained with an antibody recognizing the HA epitope encoded in the Nub tag. *B*, SDS-solubilized membrane extracts of yeast cells expressing WT or mutant Nub-Cdc50 carrying a C80A or C176A substitution were labeled with either varying amounts of mPEG or DMSO (0 μM mPEG) and subjected to immunoblot analysis using an α-HA antibody. The *arrowheads* indicate mPEG adducts of Cdc50.

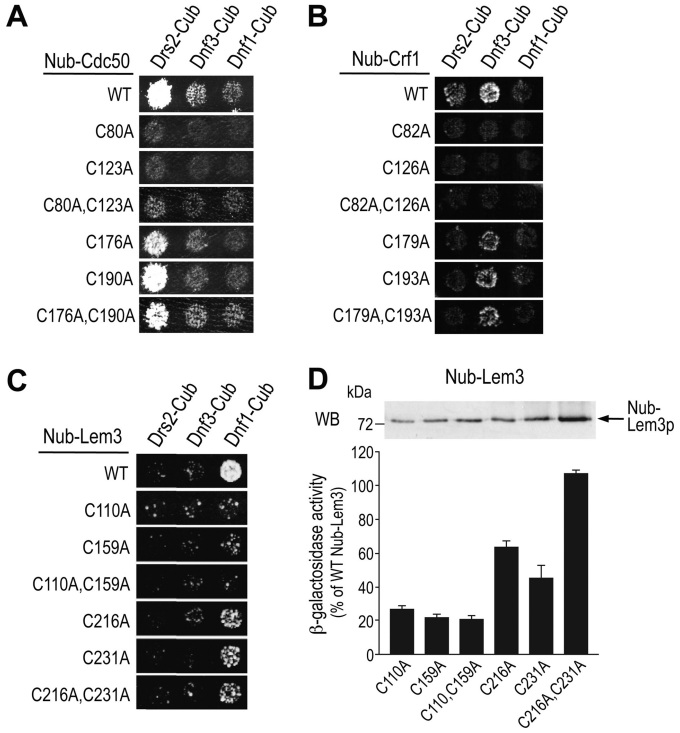

FIGURE 8. **The N-terminal disulfide bridge in the Cdc50 ectodomain is critical for P_4-ATPase binding.** Shown is a split-ubiquitin growth assay reporting interactions between Cub-tagged P_4-ATPases and Nub-tagged wild type (*WT*) as well as cysteine substitution mutants of Cdc50 (*A*), Crf1 (*B*), and Lem3 (*C*), respectively. *D*, quantitative measurement of Dnf1-Cub interactions with WT or mutant Nub-Lem3 using the β-galactosidase assay. Data shown are means ± range (*error bars*) of two independent experiments. Membrane extracts from equal amounts of cells expressing WT or mutant Nub-Lem3 were subjected to immunoblot analysis (*WB*) using an α-HA antibody.

mPEG. This experiment confirms the conclusion drawn from the mobility shift assay above and is readily applied to the C-terminal pair of cysteines. We therefore analyzed a mutation of one of the residues in that pair, C176A. As shown in the *right panel* of Fig. 7*B*, treatment of this mutant with mPEG also resulted in the appearance of multiply tagged protein (*top two arrowheads*) at the entire expense of the singly modified adduct (*bottom arrowhead*). This mutation thus makes a highly reactive third sulfhydryl (Cys^{190}) available for reaction, indicating that Cys^{176} is also involved in a disulfide bridge. From these results, we conclude that Cys^{80} pairs with Cys^{123} and Cys^{176} pairs with Cys^{190} to form two disulfide bridges in the ectodomain of Cdc50. The conservation of these residues implies that these two disulfide bridges are a conserved feature of the ectodomain structural fold.

Disruption of Disulfide Bridges in Cdc50 Subunits Has Reciprocal Effects on P_4-ATPase Binding and Function—To investigate whether disulfide bridge formation in Cdc50 subunits is relevant for P_4-ATPase binding, we first analyzed Cdc50 cysteine mutants for their interaction with Drs2 in the split-ubiquitin assay. Mutation of either one or both residues of the N-terminal Cys^{80}-Cys^{123} pair strongly reduced interaction with Drs2 as assayed by growth on selective plates (Fig. 8*A*). In contrast, disruption of the C-terminal Cys^{176}-Cys^{190} pair had only a modest effect on Drs2 binding. Likewise, mutation of the N-terminal pair of cysteine residues in Crf1 and Lem3 virtually abolished Dnf3 and Dnf1 binding, respectively, whereas mutation of the C-terminal pair affected transporter binding only to a minor extent (Fig. 8, *B* and *C*). These results were confirmed by quantitative measurements of β-galactosidase activity (Fig. 8*D*) (data not shown), demonstrating that disruption of the disulfide bridge between the N-terminal pair of cysteine residues in the ectodomain of Cdc50 subunits significantly weakens the interaction with the P_4-ATPase transporter.

We next investigated the impact of disrupting disulfide bridges in Cdc50 subunits on P_4-ATPase function. To this end, we focused on the cysteine mutants of Lem3 because this subunit forms a complex with Dnf1 and Dnf2, two plasma membrane-resident P_4-ATPases responsible for catalyzing the inward translocation of phosphatidylethanolamine (PE) and phosphatidylcholine (PC) at the cell surface (6). As expected,

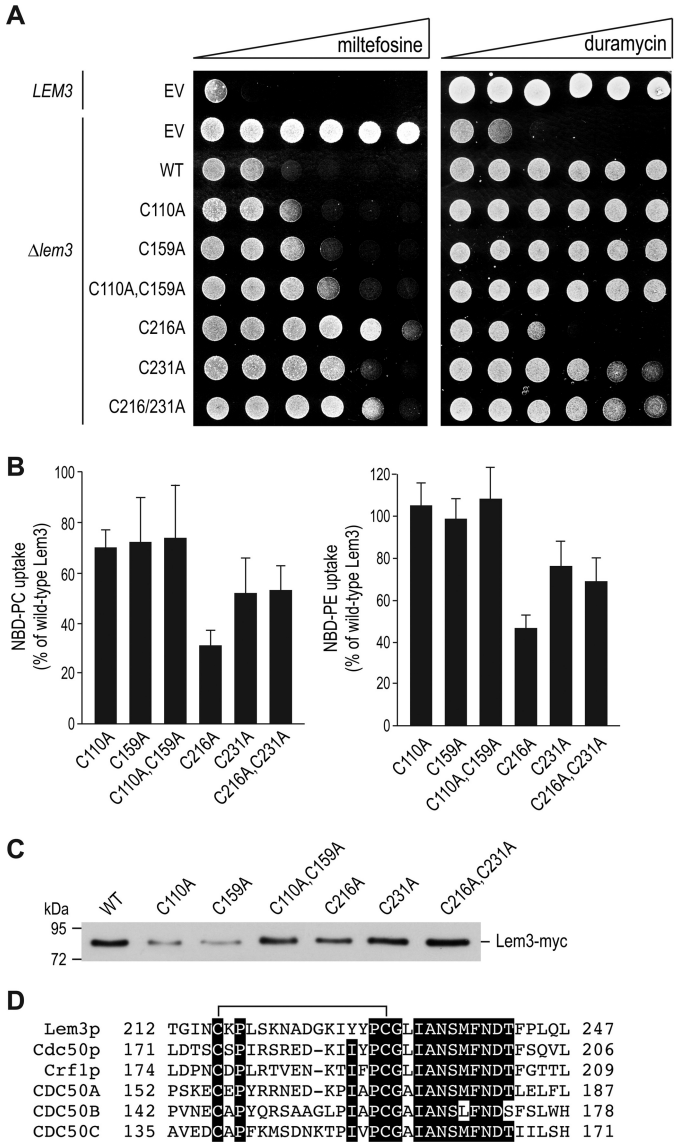

FIGURE 9. **Disruption of disulfide bridges in Cdc50 subunits differentially affects P_4-ATPase-catalyzed phospholipid transport.** *A*, Wild type (*LEM3*) and Δ*lem3* mutant strains transformed with empty vector (*EV*) or a plasmid encoding Myc-tagged wild type (*WT*) or cysteine mutants of Lem3 were spotted onto SD plates containing a concentration gradient of miltefosine or duramycin and incubated at 30 °C for 3 days. *B*, cell surface uptake of NBD-PC or NBD-PE by Δ*lem3* mutant strains expressing Myc-tagged WT or cysteine mutants of Lem3 as in *A*. NBD-phospholipid uptake was determined by flow cytometry and expressed as percentage fluorescence intensity relative to the strain expressing WT Lem3-Myc. The mean fluorescence intensity of six independent experiments was used to analyze the statistical significance by Student's *t* test. Data shown are the means ± S.D. *C*, expression levels of Myc-tagged Lem3 in the strains used for lipid uptake experiments described in *B* were determined by immunoblot analysis with an antibody against the Myc epitope. *D*, sequence alignment of Cdc50 protein family members. Only the region around the C-terminal disulfide bridge-forming cysteine pair in the ectodomain of yeast Lem3, Cdc50, and Crf1 and human CDC50A, CDC50B, and CDC50C is shown. Highly conserved residues are *shaded* in *black*.

the removal of Lem3 rendered cells resistant to the cytotoxic PC analog miltefosine and hypersensitive to the PE-binding cytotoxin duramycin (33, 34) (Fig. 9*A*). In contrast, mutation of either one or both residues of the N-terminal Cys^{110}-Cys^{159} pair in Lem3 did not affect duramycin sensitivity and caused only a minor increase in miltefosine resistance. In line with this, mutation of the Cys^{110}-Cys^{159} pair in Lem3 did not interfere with the inward translocation of NBD-labeled PE at the cell surface and caused at best only a minor (less than 30%) reduction in the inward translocation of NBD-PC (Fig. 9*B*). These findings were unexpected because disruption of the N-terminal disulfide bridge in Cdc50 subunits greatly impairs their interaction with the P_4-ATPase transporters (Fig. 8). Thus, formation of the N-terminal disulfide bridge in the Cdc50 ectodomain, although critical for P_4-ATPase binding, appears largely dispensable for P_4-ATPase-catalyzed phospholipid transport.

Mutation of the C-terminal Cys^{216}-Cys^{231} pair in Lem3 produced very different results. To begin with, substitution of Cys^{216} for Ala caused a substantial increase in miltefosine resistance and duramycin sensitivity (Fig. 9*A*), which was coupled to a major reduction in the inward translocation of NBD-PC (70%) and NBD-PE (55%) at the cell surface (Fig. 9*B*). This was surprising because mutation of Cys^{216} had only a modest effect on P_4-ATPase binding (Fig. 8, *C* and *D*). Unexpectedly, mutation of Cys^{231} had a less severe impact on miltefosine resistance and duramycin sensitivity (Fig. 9*A*), and this was reflected by a lower reduction in the inward translocation of NBD-PC (45%) and NBD-PE (25%; Fig. 9*B*). Moreover, the greater reduction in Lem3 function resulting from mutation of Cys^{216} could be alleviated by additional elimination of Cys^{231}; this effect was independent of the expression levels of the mutants (Fig. 9*C*) or their ability to associate with their P_4-ATPase binding partner (Fig. 8, *C* and *D*). Together, these results indicate that the greater reduction in Lem3 function observed upon elimination of Cys^{216} is not the result of conformational changes from disruption of the C-terminal disulfide bond. Instead, the additional inhibition appears to be a consequence of the generation of a free sulfhydryl group at the second position. As shown in Fig. 9*D*, the second cysteine in the C-terminal disulfide bond forms part of a 13-residue-long sequence motif that is nearly perfectly conserved among Cdc50 proteins from humans to yeast.

In sum, our functional analysis of Cdc50 mutants demonstrates an inverse relationship between Cdc50 binding and transport activity of P_4-ATPases. This implies that binding *per se* is not the key contribution that Cdc50 subunits make to P_4-ATPase function. Instead, our data indicate that P_4-ATPase-catalyzed phospholipid transport critically relies on a dynamic association between subunit and transporter.

DISCUSSION

Although most P-type ATPases transport small cations, P_4-ATPases are a notable exception; their known substrates are large amphipathic phospholipid molecules. Many aspects of the mechanism coupling ATP hydrolysis to substrate transport are known for the cation transporters. How this mechanism is modified to allow phospholipid transport is poorly understood. The presence of several key signature sequences in the P and A domains imply that the basic coupling of ATP hydrolysis to conformational transitions between the E_1 and E_2 conformations. But these events in the reaction cycle do not provide any information on the role of the Cdc50 proteins; recent experiments have suggested that these proteins are essential accessory subunits (19, 22, 24) and that they play a dynamic, and not just a structural, role in the reaction (19). We here set out to

identify the parts of the subunit that interact with the transporter and to define the location of the critical determinants of P_4-ATPase binding specificity. We used site-directed mutagenesis of four conserved cysteines in the ectodomain of the subunit to show that these residues form two highly conserved disulfide bridges. We also took advantage of having separate assays for binding and activity to dissect the relationship between Cdc50 binding and P_4-ATPase-catalyzed phospholipid transport. Together, the results indicate that the strength of interaction between Cdc50 proteins and their P_4-ATPase binding partners is not the only determinant of their contribution to activity, as would be predicted from their dynamic role in the phospholipid transport reaction.

Analogy with the β Subunit of Na^+/K^+-ATPases—Besides P_4-ATPases, one other notable subfamily of P-type ATPases is known to have a mandatory subunit, namely the P_{2C} subfamily of Na^+/K^+- and H^+/K^+-ATPases (13). These enzymes have been crystallized as complexes with two smaller subunits (β and γ). Interactions between the subunits and the transporting P_{2C}-ATPases include extensive contacts in the transmembrane domains and, more prominently, extensive interactions with the large extracellular domain of the β subunit, which forms a lid that completely covers the extracellular loops between M5 and M6 and between M7 and M8 (30, 35). The data presented here suggest that the overall architecture of the subunits associated with the P_4-ATPases is similar. The random mutagenesis experiments show that conserved residues scattered throughout the subunit contribute to the interaction. The domain-swapping experiments were designed to identify the location of the specific interactions that partition individual members of the Cdc50 to interactions with specific P_4-ATPases in yeast. Our observation that swapping the ectodomains between Cdc50 and Crf1 leads to a complete switch of P_4-ATPase-binding partners provides compelling evidence that this region harbors a key determinant of P_4-ATPase binding specificity. However, exchanging parts within the ectodomain produced chimeras that either lost the ability to bind any P_4-ATPase or failed to discriminate between different P_4-ATPases. This suggests that binding specificity is not mediated by a discrete region in the ectodomain but rather relies on a precise conformation of the ectodomain. Rather, these attempts to narrow the potential location of these determinants showed that there are extensive contacts between the ectodomain and the external loops of the transporter. The overall structure picture that emerges from these studies is quite similar to that observed for the P_{2C}-ATPases.

The resemblance between the subunits of the P_4- and P_{2C}-ATPases even extends to the presence of critical disulfide bonds that stabilize the ectodomain structure. The presence of these cysteines in vertebrate subunits suggests that the disulfide bonds demonstrated here have been conserved, at least since the divergence of the animals and fungi.

The Cdc50 Ectodomain as Critical Mediator of P_4-ATPase Binding and Function—The view of subunit/transporter interactions obtained from crystallography is inherently static. However, in previous work, we showed that the affinity of Cdc50 subunits for P_4-ATPases is not static but fluctuates during the ATPase reaction cycle, with the strongest interaction occurring at a point where the enzyme is loaded with phospholipid ligand (19). At first glance, these observations would suggest that strong binding affinity would be a determinant of functional efficiency. Because the experiments presented here use separate assays for binding interactions and function, this supposition could be tested, and it was found to be false. On the one hand, we found that subunits could retain the ability to bind P_4-ATPases but still be unable to render P_4-ATPases transport-competent. For instance, a Crf1-based chimera carrying the N-terminal one-third of the Cdc50 ectodomain was able to associate with native Cdc50 binding partner Drs2 in an ATPase reaction cycle-dependent manner. However, this interaction was not productive because the resulting complex did not support Drs2-catalyzed PS transport. Strikingly, swapping either the N- or C-terminal membrane span and cytosolic tail of the Crf1-based chimera for that of Cdc50 was sufficient to restore functionality. These data suggest that functionality in P_4-ATPase/Cdc50 interactions relies on cooperativity between topologically distinct domains in the Cdc50 subunit.

Even further, the data on subunits in which the two highly conserved disulfide bridges have been disrupted show that weaker interactions between subunit and transporter can support function better than more strongly interacting variants. In particular, breaking the N-terminal disulfide bond caused a dramatic reduction in the affinity of the subunit for its cognate P_4-ATPase binding partner while having only a mild effect on P_4-ATPase flippase activity. In contrast, breaking the C-terminal disulfide bond had a much smaller effect on P_4-ATPase affinity but resulted in a substantial reduction in P_4-ATPase flippase activity. Together, these results indicate that a dynamic association between subunit and transporter is crucial for the transport reaction cycle of the heterodimer.

One curious result from these studies is the greater reduction in protein function resulting from elimination of the first of the two cysteines in the C-terminal disulfide pair in comparison with elimination of the second residue or both. The latter control shows that the effect is not the result of conformation changes from disruption of the disulfide link. Instead, the additional inhibition seems to be a consequence of the generation of a free sulfhydryl at the second position. The second cysteine in the C-terminal disulfide bond forms part of a 13-residue-long sequence motif, P*C*GLIANSMFNDT, which is nearly perfectly conserved among Cdc50 proteins from humans to yeast. Our previous work suggested that Cdc50 proteins preferentially interact with the E_2P state of the P_4-ATPase (19) and thus that Cdc50 proteins may serve a crucial role in loading P_4-ATPases with phospholipid ligand. Although more experiments will be needed to understand this result in molecular terms, one possible explanation for the inhibitory effect of a free sulfhydryl at the second position is that creation of a hydrogen bond donor at this location might hold the phospholipid substrate at the external surface, resulting in less efficient translocation of the substrate to the cytoplasmic leaflet.

This result may also help explain the recent observation by Popescu and co-workers (36) that an antibody to extracellular protein-disulfide isomerase reduces the rate of PS internalization in endothelial cells, suggesting that protein-disulfide isomerase is essential for maintaining an active aminophospho-

lipid translocase. The membrane topology of P_4-ATPases and their Cdc50 binding partners indicates that the Cdc50 ectodomain provides the sole cysteine-containing region of the heteromeric complex accessible to extracellular protein-disulfide isomerase. In view of our current data, it would be interesting to investigate whether protein-disulfide isomerase-mediated preservation of the highly conserved C-terminal disulfide bridge in the Cdc50 ectodomain helps to maintain P_4-ATPase-catalyzed phospholipid transport.

Acknowledgment—We thank Maarten Egmond for stimulating discussions and critical reading of the manuscript.

REFERENCES

1. Kühlbrandt, W (2004) Biology, structure and mechanism of P-type ATPases. *Nat. Rev. Mol. Cell Biol.* **5,** 282–295
2. Bublitz, M., Morth, J. P., and Nissen P. (2011) P-type ATPases at a glance. *J. Cell Sci.* **124,** 2515–2519
3. Tang, X., Halleck, M. S., Schlegel, R. A., and Williamson, P. (1996) A subfamily of P-type ATPases with aminophospholipid transporting activity. *Science* **272,** 1495–1497
4. Coleman, J. A., Kwok, M. C., and Molday, R. S. (2009) Localization, purification, and functional reconstitution of the P4-ATPase Atp8a2, a phosphatidylserine flippase in photoreceptor disc membranes. *J. Biol. Chem.* **284,** 32670–32679
5. Zhou, X., and Graham, T. R. (2009) Reconstitution of phospholipid translocase activity with purified Drs2p, a type-IV P-type ATPase from budding yeast. *Proc. Natl. Acad. Sci. U.S.A.* **106,** 16586–16591
6. Pomorski, T., Lombardi, R., Riezman, H., Devaux, P. F., van Meer, G., and Holthuis, J. C. (2003) Drs2p-related P-type ATPases Dnf1p and Dnf2p are required for phospholipid translocation across the yeast plasma membrane and serve a role in endocytosis. *Mol. Biol. Cell* **14,** 1240–1254
7. Alder-Baerens, N., Lisman, Q., Luong, L., Pomorski, T., and Holthuis, J. C. (2006) Loss of P4 ATPases Drs2p and Dnf3p disrupts aminophospholipid transport and asymmetry in yeast post-Golgi secretory vesicles. *Mol. Biol. Cell* **17,** 1632–1642
8. Chen, S., Wang, J., Muthusamy, B. P., Liu, K., Zare, S., Andersen, R. J., and Graham, T. R. (2006) Roles for the Drs2p-Cdc50p complex in protein transport and phosphatidylserine asymmetry of the yeast plasma membrane. *Traffic* **7,** 1503–1517
9. Lenoir, G., Williamson, P., and Holthuis, J. C. (2007) On the origin of lipid asymmetry. The flip side of ion transport. *Curr. Opin. Chem. Biol.* **11,** 654–661
10. Puts, C. F., and Holthuis, J. C. (2009) Mechanism and significance of P4 ATPase-catalyzed lipid transport. Lessons from a Na^+/K^+-pump. *Biochim. Biophys. Acta* **1791,** 603–611
11. Baldrigde, R. D., and Graham, T. R. (2012) Identification of residues defining phospholipid flippase substrate specificity of type IV P-type ATPases. *Proc. Natl. Acad. Sci. U.S.A.* **109,** E290–E298
12. Coleman, J. A., Vestergaard, A. L., Molday, R. S., Vilsen, B., and Peter Andersen, J. (2012) Critical role of a transmembrane lysine in aminophospholipid transport by mammalian photoreceptor P4-ATPase ATP8A2. *Proc. Natl. Acad. Sci. U.S.A.* **109,** 1449–1454
13. Geering, K. (2008) Functional roles of Na,K-ATPase subunits. *Curr. Opin. Nephrol. Hypertens.* **17,** 526–532
14. Poulsen, L. R., López-Marqués, R. L., and Palmgren, M. G. (2008) Flippases. Still more questions than answers. *Cell. Mol. Life Sci.* **65,** 3119–3125
15. Hua, Z., Fatheddin, P., and Graham, T. R. (2002) An essential subfamily of Drs2p-related P-type ATPases is required for protein trafficking between Golgi complex and endosomal/vacuolar system. *Mol. Biol. Cell* **13,** 3162–3177
16. Wicky, S., Schwarz, H., and Singer-Krüger, B. (2004) Molecular interactions of yeast Neo1p, an essential member of the Drs2 family of aminophospholipid translocases, and its role in membrane trafficking within the endomembrane system. *Mol. Cell. Biol.* **24,** 7402–7418
17. Saito, K., Fujimura-Kamada, K., Furuta, N., Kato, U., Umeda, M., and Tanaka, K. (2004) Cdc50p, a protein required for polarized growth, associates with the Drs2p P-type ATPase implicated in phospholipid translocation in *Saccharomyces cerevisiae*. *Mol. Biol. Cell* **15,** 3418–3432
18. Furuta, N., Fujimura-Kamada, K., Saito, K., Yamamoto, T., and Tanaka, K. (2007) Endocytic recycling in yeast is regulated by putative phospholipid translocases and the Ypt31p/32p-Rcy1p pathway. *Mol. Biol. Cell* **18,** 295–312
19. Lenoir, G., Williamson, P., Puts, C. F., and Holthuis, J. C. (2009) Cdc50p plays a vital role in the ATPase reaction cycle of the putative aminophospholipid transporter Drs2p. *J. Biol. Chem.* **284,** 17956–17967
20. Kato, U., Emoto, K., Fredriksson, C., Nakamura, H., Ohta, A., Kobayashi, T., Murakami-Murofushi, K., and Umeda, M. (2002) A novel membrane protein, Ros3p, is required for phospholipid translocation across the plasma membrane in Saccharomyces cerevisiae. *J. Biol. Chem.* **277,** 37855–37862
21. Paulusma, C. C., Folmer, D. E., Ho-Mok, K. S., de Waart, D. R., Hilarius, P. M., Verhoeven, A. J., and Oude Elferink, R. P. (2008) ATP8B1 requires an accessory protein for endoplasmic reticulum exit and plasma membrane lipid flippase activity. *Hepatology* **47,** 268–278
22. Bryde, S., Hennrich, H., Verhulst, P. M., Devaux, P. F., Lenoir, G., and Holthuis, J. C. (2010) CDC50 proteins are critical components of the human class-1 P4-ATPase transport machinery. *J. Biol. Chem.* **285,** 40562–40572
23. van der Velden, L. M., Wichers, C. G., van Breevoort, A. E., Coleman, J. A., Molday, R. S., Berger, R., Klomp, L. W., and van de Graaf, S. F. (2010) Heteromeric interactions required for abundance and subcellular localization of human CDC50 proteins and class 1 P4-ATPases. *J. Biol. Chem.* **285,** 40088–40096
24. Coleman, J. A., and Molday, R. S. (2011) Critical role of the β-subunit CDC50A in the stable expression, assembly, subcellular localization, and lipid transport activity of the P4-ATPase ATP8A2. *J. Biol. Chem.* **286,** 17205–17216
25. Takahashi, Y., Fujimura-Kamada, K., Kondo, S., and Tanaka, K. (2011) Isolation and characterization of novel mutations in CDC50, the noncatalytic subunit of the Drs2p phospholipid flippase. *J. Biochem.* **149,** 423–432
26. Jacquot, A., Montigny, C., Hennrich, H., Barry, R., le Maire, M., Jaxel, C., Holthuis, J., Champeil, P., and Lenoir, G. (2012) Phosphatidylserine stimulation of Drs2p·Cdc50p lipid translocase dephosphorylation is controlled by phosphatidylinositol-4-phosphate. *J. Biol. Chem.* **287,** 13249–13261
27. Krogh, A., Larsson, B., von Heijne, G., and Sonnhammer, E. L. (2001) Predicting transmembrane protein topology with a hidden Markov model. Application to complete genomes. *J. Mol. Biol.* **305,** 567–580
28. Larkin, M. A., Blackshields, G., Brown, N. P., Chenna, R., McGettigan, P. A., McWilliam, H., Valentin, F., Wallace, I. M., Wilm, A., Lopez, R., Thompson, J. D., Gibson, T. J., and Higgins, D. G. (2007) ClustalW and ClustalX version 2.0. *Bioinformatics* **23,** 2947–2948
29. Obrdlik, P., El-Bakkoury, M., Hamacher, T., Cappellaro, C., Vilarino, C., Fleischer, C., Ellerbrok, H., Kamuzinzi, R., Ledent, V., Blaudez, D., Sanders, D., Revuelta, J. L., Boles, E., Andre, B., and Frommer, W. B. (2004) K+ channel interactions detected by a genetic system optimized for systematic studies of membrane protein interactions. *Proc. Natl. Acad. Sci. U.S.A.* **101,** 12242–12247
30. Shinoda, T., Ogawa, H., Cornelius, F., and Toyoshima, C. (2009) Crystal structure of the sodium-potassium pump at 2.4 Å resolution. *Nature* **459,** 446–450
31. Grefen, C., Lalonde, S., and Obrdlik, P. (2007) Split-ubiquitin system for identifying protein-protein interactions in membrane and full-length proteins. *Curr. Protoc. Neurosci.* Chapter 5, Unit 5.27
32. Parsons, A. B., Lopez, A., Givoni, I. E., Williams, D. E., Gray, C. A., Porter, J., Chua, G., Sopko, R., Brost, R. L., Ho, C. H., Wang, J., Ketela, T., Brenner, C., Brill, J. A., Fernandez, G. E., Lorenz, T. C., Payne, G. S., Ishihara, S., Ohya, Y., Andrews, B., Hughes, T. R., Frey, B. J., Graham, T. R., Andersen, R. J., and Boone, C. (2006) Exploring the mode-of-action of bioactive compounds by chemical-genetic profiling in yeast. *Cell* **126,** 611–625
33. Hanson, P. K., Malone, L., Birchmore, J. L., and Nichols, J. W. (2003)

Lem3p is essential for the uptake and potency of alkylphosphocholine drugs, edelfosine and miltefosine. *J. Biol. Chem.* **278,** 36041–36050

34. Noji, T., Yamamoto, T., Saito, K., Fujimura-Kamada, K., Kondo, S., and Tanaka, K. (2006) Mutational analysis of the Lem3p-Dnf1p putative phospholipid-translocating P-type ATPase reveals novel regulatory roles for Lem3p and a carboxyl-terminal region of Dnf1p independent of the phospholipid-translocating activity of Dnf1p in yeast. *Biochem. Biophys. Res. Commun.* **344,** 323–331
35. Morth, J. P., Pedersen, B. P., Toustrup-Jensen, M. S., Sørensen, T. L., Petersen, J., Andersen, J. P., Vilsen, B., and Nissen, P. (2007) Crystal structure of the sodium-potassium pump. *Nature* **450,** 1043–1049
36. Popescu, N. I., Lupu, C., and Lupu, F. (2010) Extracellular protein-disulfide isomerase regulates coagulation on endothelial cells through modulation of phosphatidylserine exposure. *Blood* **116,** 993–1001